Weighted Correlation Gene Networks and Gene Set Enrichment Analysis Revealed New Potential Genetic Etiologies Associated with Cryptorchidism

Wenlin Huang[1], JinGe Liu[1], Ziwei Liu[1], Yong Xu[1]*

Purpose: Despite its prevalence, the etiology and pathogenesis of cryptorchidism remain poorly understood. This study aimed to identify potential biomarkers associated with cryptorchidism development using bioinformatics methodologies.

Materials and Methods: We utilized three microarray datasets from the Gene Expression Omnibus (GEO) database, comparing gene expression profiles between cryptorchidism patients and control individuals. Differentially expressed genes (DEGs) were identified using statistical analysis. Subsequently, we constructed a gene co-expression network using weighted gene co-expression network analysis (WGCNA) to identify modules of genes highly associated with the cryptorchid phenotype. Hub genes within these modules were identified using cross-validation and multiple algorithms.

Results: A total of 1,539 differentially expressed genes were identified between cryptorchidism patients and controls. WGCNA revealed a gene module strongly associated with the cryptorchidism phenotype. Ten genes (CDH1, CS, G6PD, HSPA5, KEAP1, NEDD8, POLR2J, JUN, SOD2, and TXN) with the highest association to cryptorchidism were identified in this module. Single gene gene set enrichment analysis (ssGSEA) showed that these hub genes were mainly enriched in metabolism-, translation-, and inflammation related processes. Notably, several key genes are involved in oxidative stress responses.

Conclusion: This study identified a credible set of hub genes associated with cryptorchidism. Some of these genes have been shown to affect testicular development or spermatogenesis through mechanisms such as inflammation and oxidative stress, while others have not been fully studied in the context of cryptorchidism. These hub genes may provide new biomarkers for cryptorchidism risk assessment and warrant further investigation to clarify their specific roles.

Keywords: cryptorchidism; biomarkers; genetic etiology; hub gene; inflammation

INTRODUCTION

Cryptorchidism, also known as undescended testis (UDT), is a congenital malformation characterized by the failure of testicular descent through the inguinal canal into the scrotum during normal development. It is the most prevalent congenital anomaly in male newborns, affecting approximately 1% to 9% of full term infants and up to 45% of premature infants[1,2]. Typically, the undescended testis can be palpated in the inguinal region upon physical examination; however, in certain cases, it remains within the abdominal cavity and eludes detection[3]. While cryptorchidism is primarily diagnosed through physical examination, imaging examinations are often necessary for confirmation. Orchidopexy (surgical correction of testicular descent) is the primary treatment modality. The pathogenesis of cryptorchidism is believed to be related to developmental defects[4] and can manifest as either an isolated symptom or a sign of other congenital malformations. Nevertheless, despite ongoing research, the mechanisms remain incompletely understood, underscoring a lack of effective preventive measures.

Numerous studies have explored associations between cryptorchidism and genes[5]. Emerging evidence highlights links between diverse genetic alterations (including expression dysregulation and mutations) and disease pathogenesis[6]. Therefore, the biological pathways associated with cryptorchidism require further elucidation. Multiple genes with similar biological functions or involvement in the same pathways may regulate disease occurrence and progression. For example, insulin like factor 3 (INSL3), secreted by testicular Leydig cells, is believed to influence testicular descent via mechanisms including promoting gubernaculum development[7]. UDT is also androgen dependent and may be affected by endocrine disrupting compounds (EDCs) targeting the androgen receptor (AR)[8]. Additionally, targeted knockout of WNT4 in the mouse testicular gubernaculum induces ipsilateral cryptorchidism[9]. Weighted gene co expression network analysis (WGCNA) can identify gene clusters with highly correlated expression levels, correlate them with phenotypes, and provide insights into co expressed gene functions and disease development[10,11]. In this study, we examined GEO mi-

[1]Department of Urology, Zhuzhou Hospital Affiliated to Xiangya School of Medicine, Central South University, Zhuzhou, Hunan Province, No. 116, South of Changjiang Road, Tianyuan District, 412007, China.
*Corresponding author: Department of Urology, Zhuzhou Hospital Affiliated to Xiangya School of Medicine, Central South University
Tel: +86 18670872766. E mail: tigerhnllxu2021@126.com.
Received October 2024 & Accepted November 2025

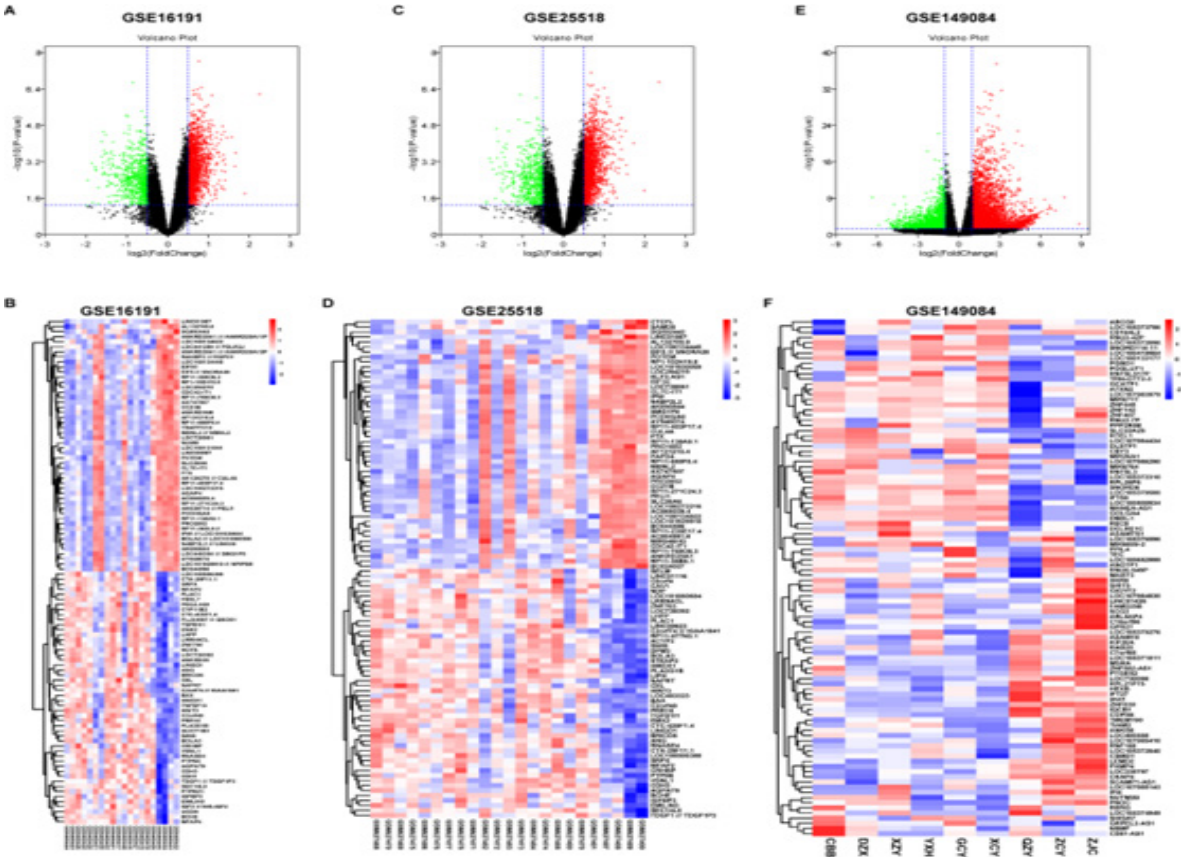

Figure 1. Identification of DEGs between biopsy specimens from patients with cryptorchidism and normal specimens. A volcano plot displays the differential gene expression data from three datasets: A. GSE149084, C. GSE16191, and E. GSE25518. Red dots indicate up regulated genes (log2FC ≥ 0.5, adjusted P < 0.05), green dots indicate down regulated DEGs, and black dots represent genes that are not significantly differentially expressed. A heat map of the top 100 DEGs from three additional datasets (B. GSE83453, D. GSE51472, F. GSE12644) shows expression levels, represented by color intensity from red (high) to blue (low).

croarray data to identify DEGs between children with cryptorchidism and healthy controls. We performed functional enrichment analyses to identify implicated biological processes and pathways, applied WGCNA to identify phenotype linked modules and candidate hub genes, and then conducted correlation based single gene GSEA. These analyses uncovered pathways related to cryptorchidism onset that could inform future diagnosis and treatment.

MATERIALS AND METHODS

Data acquisition and preprocessing

We obtained RNA expression profiling microarray data from publicly available GEO datasets: GSE149084, GSE16191, and GSE25518. In total, 52 samples were included (41 boys with cryptorchidism and 11 controls). All tissue samples were testicular biopsies. A post hoc power analysis was conducted via the pwr package in R (v3.6.1). Assuming a medium effect size (Cohen's d = 0.5) with $\alpha = 0.05$ and 80% power, the minimal required sample size was 34 (17 per group). Our cohort (n = 52) exceeds this threshold. We used limma's empirical Bayes variance moderation to enhance reliability in small sample microarray studies. Expression profiles underwent log2 transformation, background correction, and quantile normalization. Datasets were selected as large, relevant public resources for cryptorchidism to ensure sufficient power to detect meaningful differences using limma in R. DEGs between cryptorchidism and controls were identified using limma with thresholds of absolute log2 fold change > 0.5 and adjusted $P < 0.05$[12].

Functional enrichment analysis

To understand biological functions of DEGs, we conducted Gene Ontology (GO) and Kyoto Encyclopedia of Genes and Genomes (KEGG) enrichment analyses. GO included cellular component (CC), biological process (BP), and molecular function (MF). We utilized the clusterProfiler package in R (3.6.1)[13], with $P < .05$ considered significant.

Weighted gene co expression network analysis

WGCNA was used to identify association patterns among protein coding DEGs and to construct co expression networks and module clusters (R package WGCNA v1.71). A one step network constructor was employed. Datasets were evaluated for approximate scale free topology to select soft threshold power. Module eigengenes (MEs; first principal component of module expression) were correlated with clinical traits to assess module–trait relationships using Pearson's correlation; interaction was considered when r > 0.25.

Hub gene identification and single gene GSEA

Modules highly associated with cryptorchidism were subjected to enrichment analysis using clusterProfiler. Genes from these modules were used to construct a protein–protein interaction (PPI) network in STRING (http://string-db). We used Cytoscape–CytoHubba with

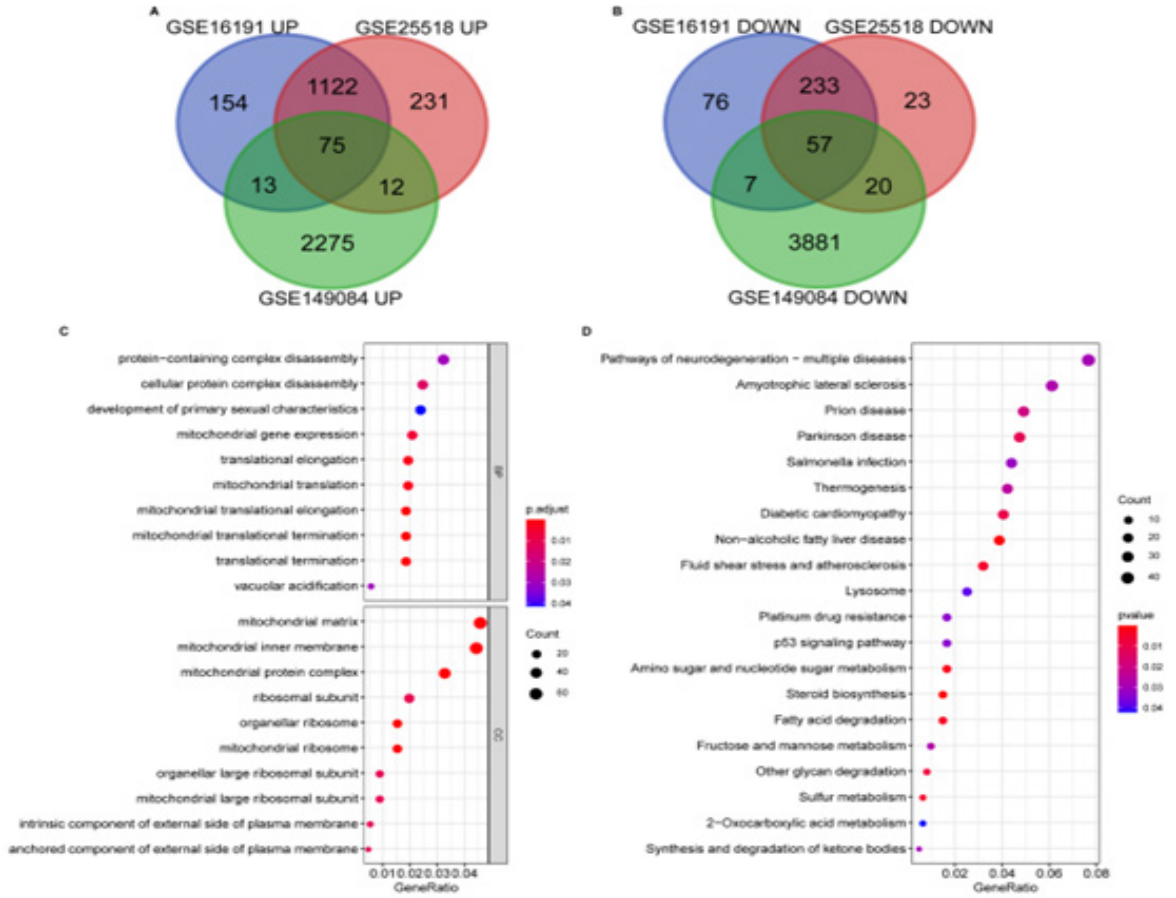

Figure 2. Enrichment analysis of differentially expressed genes (DEGs). A. Venn diagrams displaying key up-regulated DEGs overlap in GSE149084, GSE16191, and GSE2551. B. Venn diagrams displaying key down-regulated DEGs overlap in GSE149084, GSE16191, and GSE2551. C. GO enrichment analysis of DEGs with intersections across all three datasets. D. KEGG pathway enrichment analysis of DEGs with intersections across all three datasets

multiple algorithms (Degree, MNC, Radiality, Stress, Closeness) to identify the top hub genes. Correlation analysis between these hub genes and all genes in GSE16191 identified the top 50 most positively correlated genes for heat map visualization. Genes with significant correlation (P < .05) were used for single gene GSEA.

RESULTS

Identification of differentially expressed genes (DEGs)
We analyzed GSE149084, GSE16191, and GSE25518. In GSE149084 (6 cryptorchidism; 3 controls), there were 2,375 up regulated and 3,965 down regulated DEGs in cryptorchidism (**Figure 1A, 1B**). In GSE16191 (16 cryptorchidism; 4 controls), there were 2,202 up regulated and 3,348 down regulated DEGs (Figure 1C, 1D). In GSE25518 (19 cryptorchidism; 4 controls), there were 1,440 up regulated and 333 down regulated DEGs (**Figure 1E, 1F**). Thresholds were absolute log2 fold change > 0.5 and adjusted $P < 0.05$ across all datasets.

GO and KEGG pathway enrichment analysis

Across the three datasets, we obtained 75 common up regulated DEGs and 57 common down regulated DEGs. Additionally, 1,222 DEGs were up regulated in at least two datasets, and 317 were down regulated in at least two datasets (Figure 2A, 2B). GO and KEGG enrichment analyses were performed on the 1,539 DEGs (1,222 up and 317 down) (**Figure 2C, 2D**). GO analysis revealed categories related to male sexual development, including gonad development (GO:0008406), male gonad development (GO:0008584), male sex differentiation (GO:0046661), development of primary sexual characteristics (GO:0045137), and development of primary male sexual characteristics (GO:0046546). KEGG analysis highlighted pathways linked to neurodegeneration (multiple diseases), amyotrophic lateral sclerosis, prion disease, and others.

Weighted gene co expression network analysis and module identification

Hierarchical clustering confirmed the absence of outlier samples and distinguished cryptorchidism from controls (**Figure 3A**). GSE16191 was used for WGCNA. Based on scale free topology, a soft threshold power of 10 was selected (**Figure 3B**). The cryptorchidism specific co expression modules are shown in (Figure 3C). From 1,539 DEGs shared in at least two datasets, protein coding genes were clustered into four modules (MEgreen, MEpink, MEpurple, MEgrey). Module–trait analysis showed the MEpurple module had a strong positive correlation with unilateral cryptorchidism (r = 0.89; 95% CI: 0.85–0.92; $P < .001$) (**Figure 4A**). A topological overlap matrix (TOM) heat map is shown in (**Figure 4B**). The purple module (1,286 DEGs) dis-

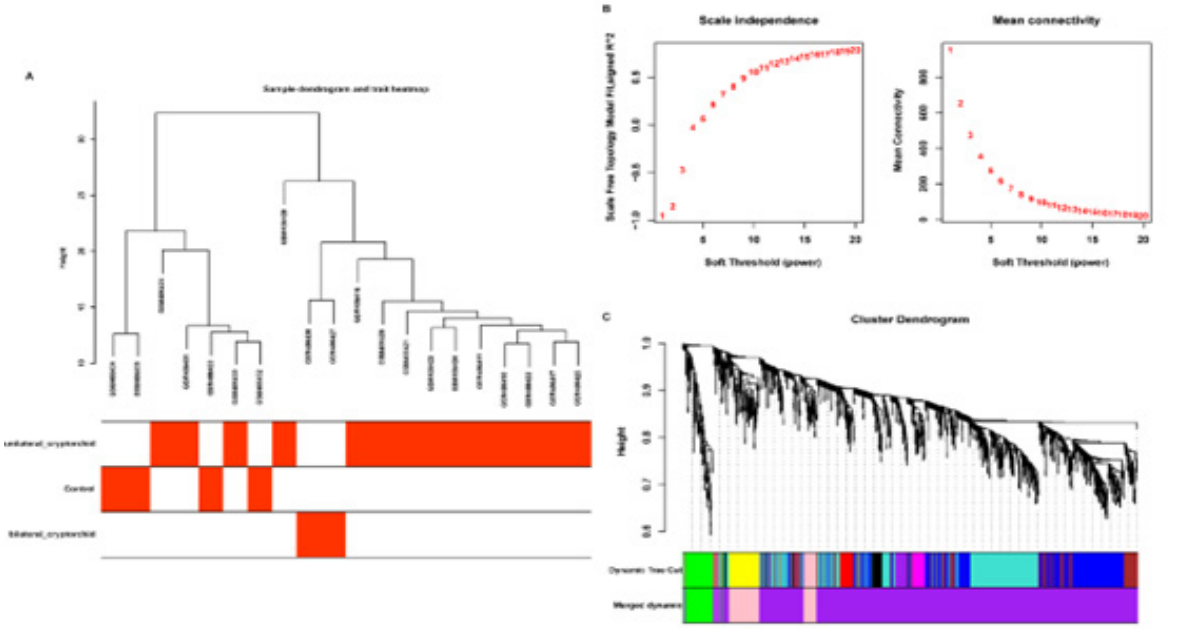

Figure 3. Sample clustering and network construction of weighted co expressed genes based on cryptorchidism. A. Clustering dendrogram of cryptorchidism and control samples; color intensity is proportional to disease state (unilateral or bilateral). B. Network topology under scale free fitting index and various soft threshold powers (scale independence and mean connectivity shown). C. Co expression modules in cryptorchidism.

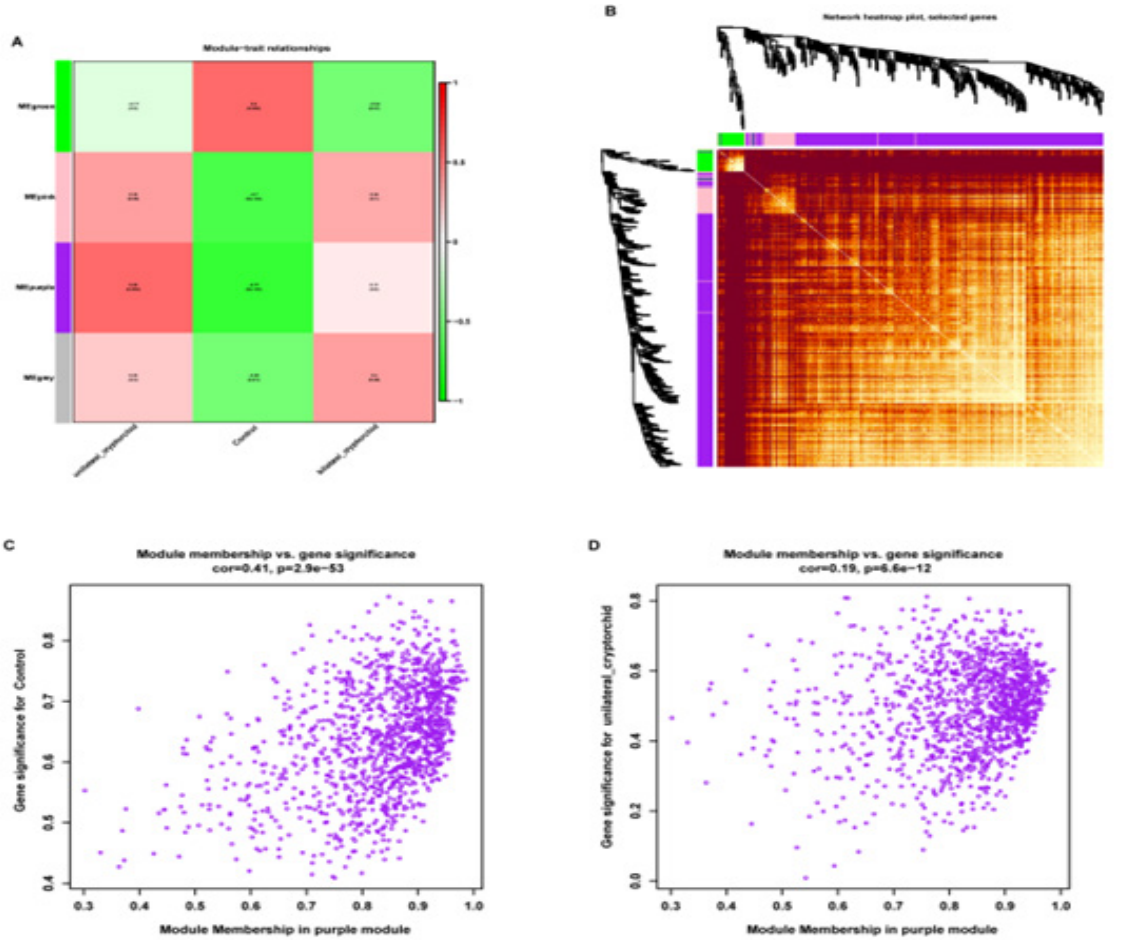

Figure 4. Key module in WGCNA. **A.** Heat map showing correlation between differential genes and cryptorchidism (cell center shows correlation coefficient and *P*-value; color reflects strength). **B.** Darker colors indicate greater overlap. **C.** Topological overlap matrix of selected protein coding genes among differential genes. **D.** Scatter plot depicting disease group and purple module.

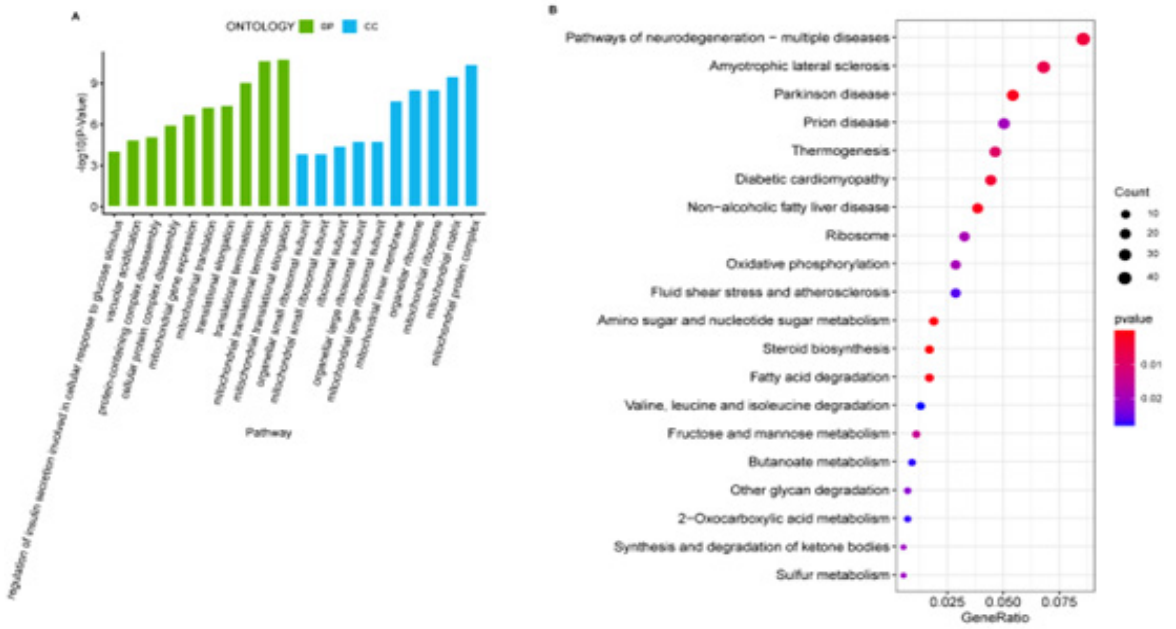

Figure 5. A. GO analysis identifying enriched biological process (BP; green bars) and cellular component (CC; blue bars) terms for genes in the purple module. **B.** KEGG analysis of genes in the purple module ($P < 0.01$; FDR < 0.05).

played the strongest association. Adjacency heat maps and scatter plots indicated strong correlations between module membership and gene significance in both cryptorchidism and control groups (r = 0.71 and r = 0.79, respectively; both $P < .001$) (**Figure 4C, 4D**).

Functional enrichment analysis of key modules

Functional enrichment of the purple module using clusterProfiler revealed enrichment in mitochondrial

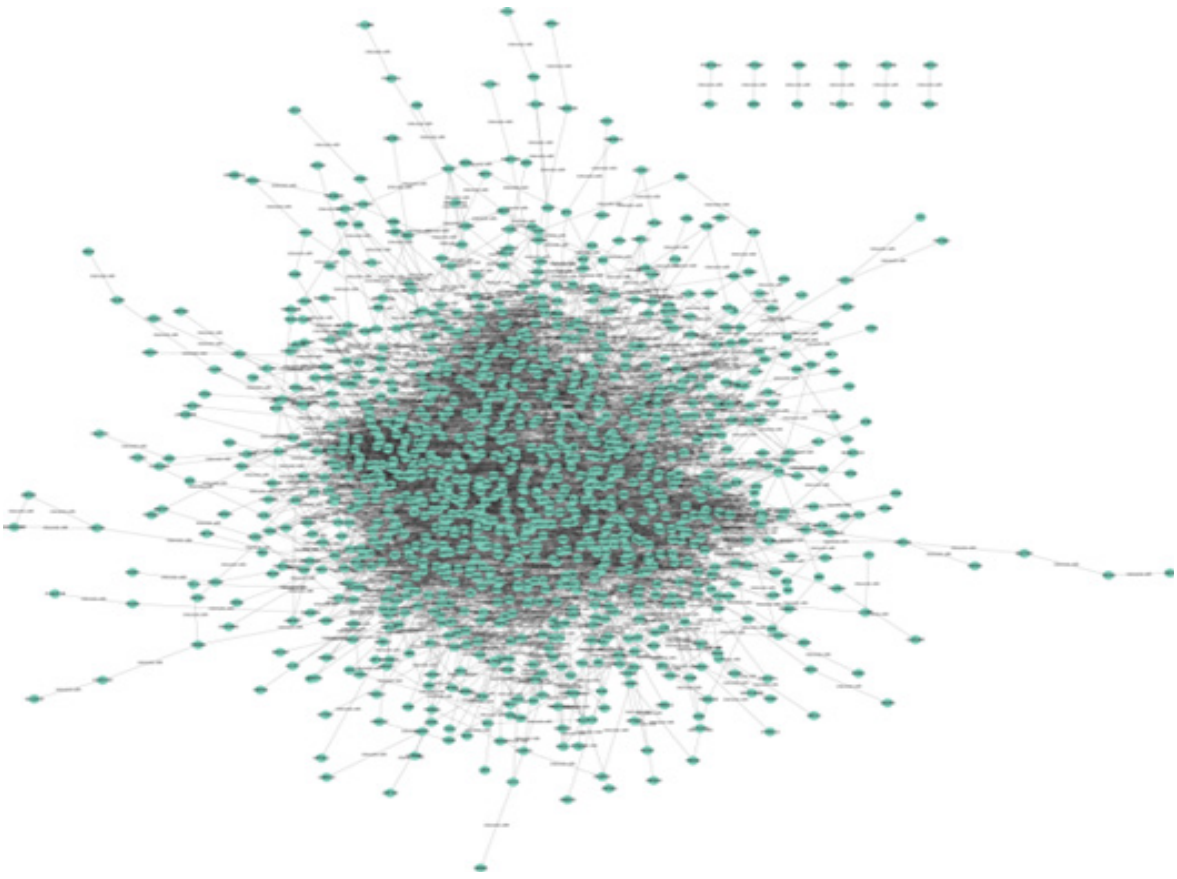

Figure 6. Protein–protein interaction (PPI) network diagram of genes in the purple module.

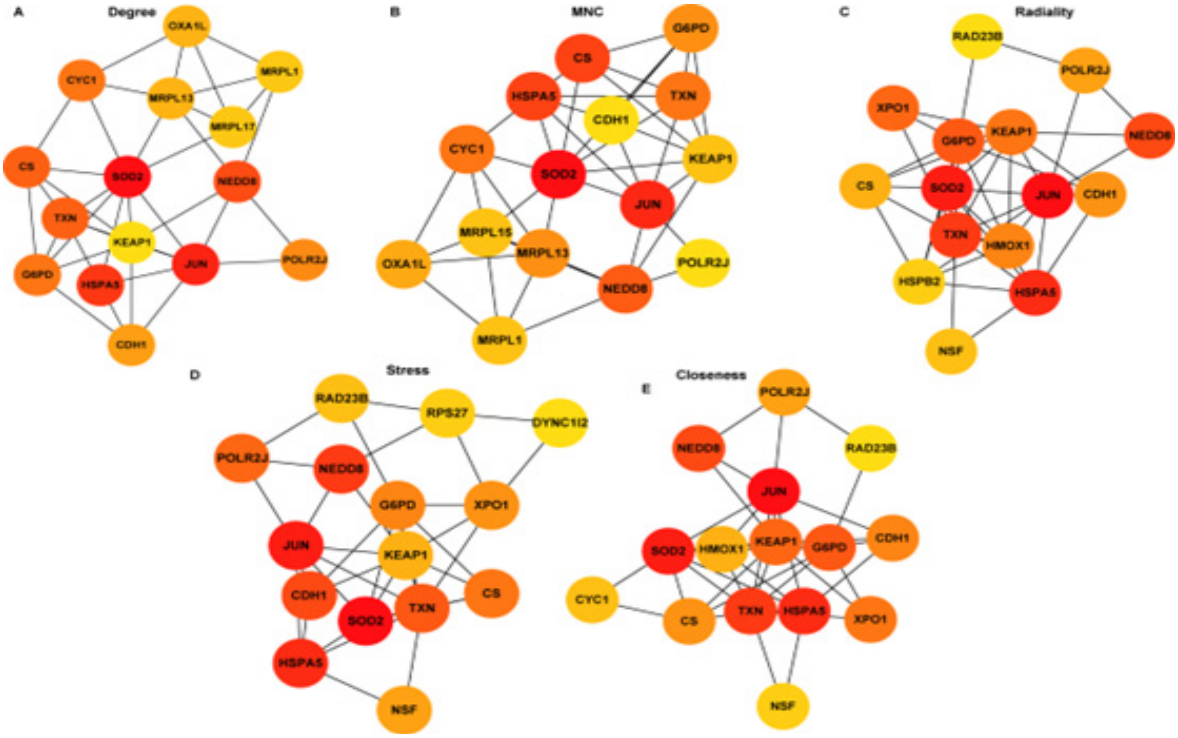

Figure 7. The most central 15 genes in the PPI network identified by five algorithms (Degree, MNC, Radiality, Stress, Closeness).

translational elongation and termination; cellular components included mitochondrial protein complexes, mitochondrial matrix, mitochondrial ribosomes, organellar ribosomes, and the mitochondrial inner membrane (**Figure 5A**). KEGG pathways showed the highest enrichment in neurodegeneration (multiple diseases),

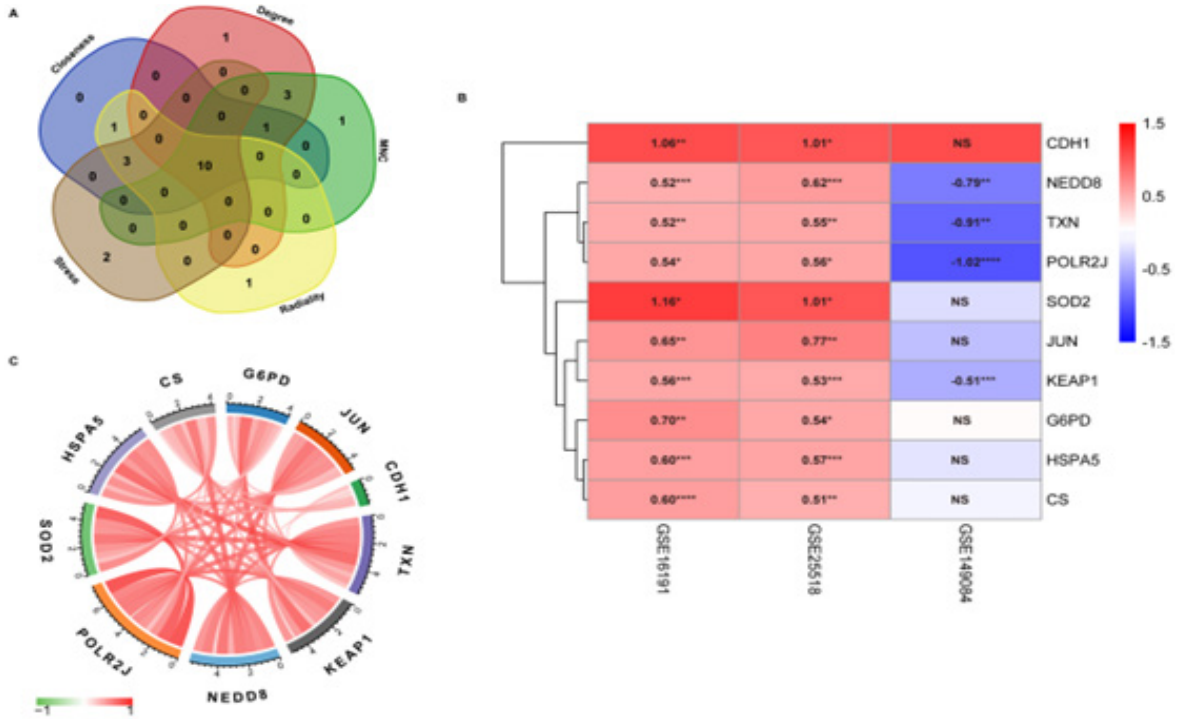

Figure 8. A. Venn diagram demonstrating intersection of hub genes identified by five different CytoHubba algorithms (Degree, MNC, Radiality, Stress, and Closeness). A total of 10 common hub genes were identified through overlapping analysis. **B.** Heatmap illustrating differential expression (Log2 fold change, Log2FC) of the 10 hub genes (CDH1, CS, G6PD, HSPA5, KEAP1, NEDD8, POLR2J, JUN, SOD2, and TXN) across three GEO datasets (GSE16191, GSE25518, and GSE149084). Values represent Log2 fold changes; exact -values are indicated (*$P < .05$; **$P < .01$; ***$P < .005$; ****$P < .001$). C. Circos plot displaying the correlation among the identified hub genes, with correlation strengths ranging from positive (red) to negative (green).correlation among the identified hub genes, with correlation strengths ranging from positive (red) to negative (green)..

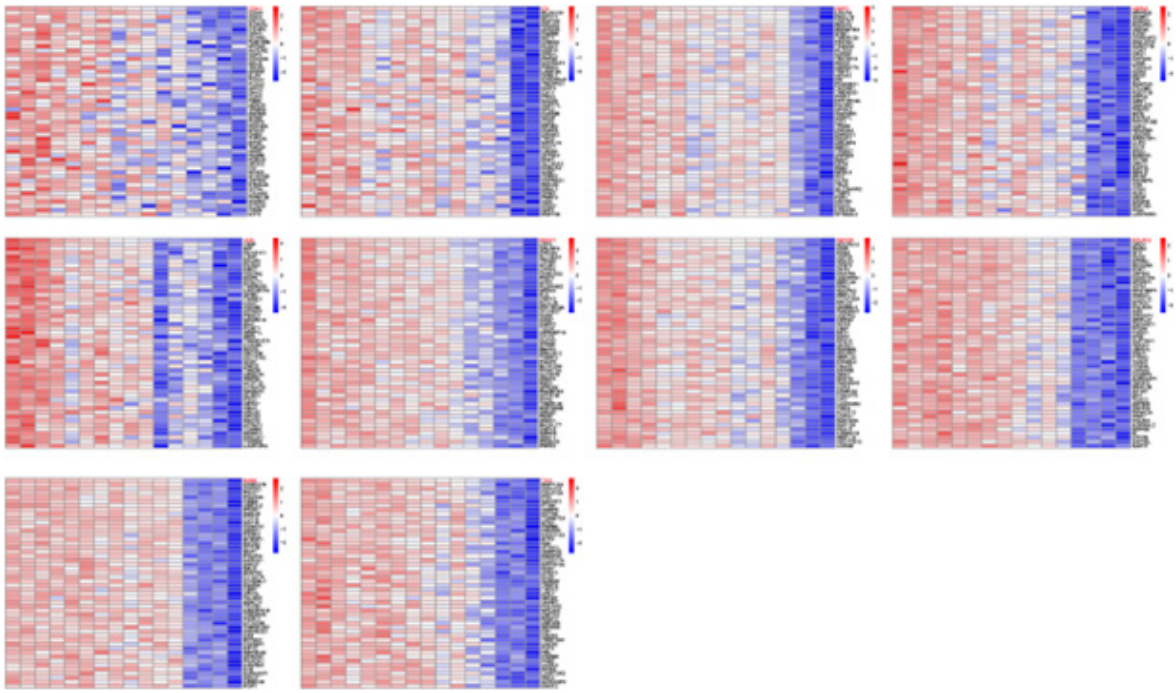

Figure 9. Based on GSE16191, correlation analyses between each of the 10 hub genes and all genes were performed. Heat maps show the top 50 genes positively correlated with each hub gene's expression.

followed by amyotrophic lateral sclerosis, Parkinson's disease, and prion disease (**Figure 5B**).

PPI network construction and hub gene identification

Genes from the purple module were imported into STRING to construct a PPI network, visualized in Cytoscape (**Figure 6**). Using five CytoHubba algorithms (Degree, MNC, Radiality, Stress, Closeness), the most central 15 genes were identified (**Figure 7**). Intersecting results yielded 10 hub genes: CDH1, CS, G6PD, HSPA5, KEAP1, NEDD8, POLR2J, JUN, SOD2, and

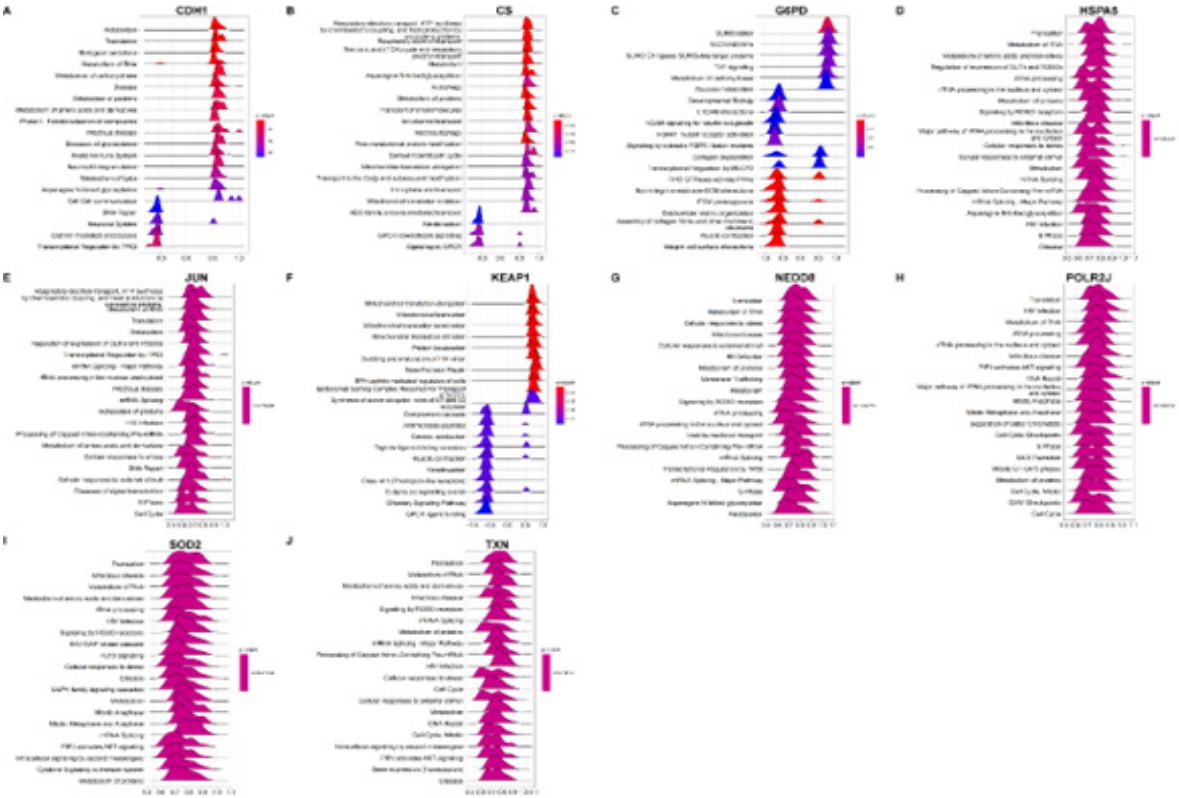

Figure 10. Results of single gene GSEA conducted separately for the 10 hub genes and genes with comparable expression patterns.

TXN (**Figure 8A**). A heat map of these hub genes across GSE149084, GSE16191, and GSE25518 is shown (Figure 8B). Correlation mapping among the 10 hub genes in GSE16191 demonstrated strong co expression patterns associated with cryptorchidism (**Figure 8C**).

Gene set enrichment analysis of hub genes

Correlation analyses between each hub gene and all other genes in GSE16191 identified the top 50 positively correlated genes for each hub gene, visualized in heat maps (**Figure 9**). These gene sets served as inputs for single gene GSEA, which demonstrated significant enrichment ($P < .05$) and provided cumulative enrichment scores for pathways associated with each hub gene (**Figure 10**).

DISCUSSION

Cryptorchidism is a common congenital malformation with unclear risk factors and pathogenesis despite clear anatomic understanding. Genetic and environmental factors can influence testicular descent[14]. Multiple studies have linked cryptorchidism to genetic etiologies[15,16]. As cryptorchidism is often a syndrome phenotype rather than an independent disease, numerous genes likely shape its occurrence and development, contributing to heterogeneity in testis location and laterality[17]. To provide robust references for future studies, we applied rigorous bioinformatic methods to GEO microarray data, using WGCNA and GSEA to identify key genes and enriched pathways related to cryptorchidism.

WGCNA groups and visualizes gene expression by converting profiles into networks, enabling construction of gene sets and pathway enrichment to identify DEGs and their biological roles. Advantages include simultaneous multi sample analysis, support for large scale research, delineation of global regulatory networks, and identification of complex pathways and feedback loops[18,19]. GSEA evaluates relationships between gene sets and phenotypes based on high throughput data, accounting for the continuous nature of gene expression and inter gene correlations; it facilitates comprehensive analysis beyond single gene thresholds[6,20].

We identified 1,539 DEGs dysregulated in at least two datasets and found enrichment in pathways related to metabolic reprogramming, translational regulation, inflammatory cascades, and oxidative stress. WGCNA pinpointed the purple module as strongly associated with cryptorchidism. This is consistent with the view that cryptorchidism's etiology is multifactorial and pathway based rather than driven by single genes[17]. We identified 10 hub genes—CDH1, CS, G6PD, HSPA5, KEAP1, NEDD8, POLR2J, JUN, SOD2, and TXN—implicated in testicular development, sperm morphology and number, metabolism, and inflammation. Single gene GSEA showed predominant enrichment in metabolism (protein, carbohydrate, RNA), translation, and inflammatory processes.

HSPA5 (GRP78), a heat shock protein involved in endoplasmic reticulum stress response[23], may modulate Leydig cell function during testicular development; activation of the GRP78(HSPA5)/IRE1 pathway after oxidative stress and DNA damage can inhibit testosterone synthesis[24]. Overexpression can induce testicular inflammation, morphological alterations, and reduced sperm count[25]. JUN encodes an AP 1 subunit involved in growth, differentiation, and apoptosis[26]; AP 1 participates in Leydig cell communication and interacts with AR via androgen mediated regulation[27–29], potentially influencing cryptorchidism. SOD2, a key antioxidant enzyme, has been implicated in sperm activation in Caenorhabditis elegans[30]; oxidative imbalance can contribute to testicular hypoplasia syndromes, including cryptorchidism[31]. KEAP1, central to the NRF2/KEAP1 pathway[32], may be protective in cryptorchidism. NEDD8, a ubiquitin like modifier regulating proteostasis via neddylation, may affect androgen receptor signaling through ubiquitin proteasome mediated control of AR stability and activity[33].

Our approach moved beyond DEG identification to modular analysis of a gene set strongly associated with the cryptorchidism phenotype, identifying genes with coherent expression patterns and their enrichment directionality—potentially informing future functional work. Challenges include the practical and ethical difficulty of obtaining healthy testicular tissues as controls; thus, we relied on public datasets for preliminary bioinformatics analyses. Nonetheless, rigorous analyses can provide valuable guidance for subsequent investigations.

CONCLUSIONS

This study leveraged WGCNA and GSEA to delineate genetic etiologies and inflammatory pathways implicated in cryptorchidism. Integrated analyses of three GEO microarray datasets identified 1,539 DEGs enriched in metabolic, translational, inflammatory, and oxidative stress pathways. Hub genes including HSPA5, JUN, SOD2, and KEAP1 appear to orchestrate critical processes linked to testicular development and spermatogenic function. Single gene GSEA supported their roles in cryptorchidism associated pathways. Future studies should prioritize in vivo functional validation to dissect tissue specific roles in gubernaculum development and androgen responsiveness, with the goal of identifying potential therapeutic targets for mitigating UDT.

SUMMARY

Using public gene data and network analyses, we identified 10 key genes and several pathways (metabolism, inflammation, oxidative stress) linked to undescended testis. These findings may help improve diagnosis and guide future treatments.

CONFLICT OF INTEREST

The authors report no conflict of interest.

FUNDING

This work was supported by the Hunan Provincial Natural Science Foundation of China (Grant numbers: 2023JJ41065, 2020JJ8054).

DATA AVAILABILITY

All data for this study are available from the GEO databases (GSE149084, GSE16191, GSE25518).

AUTHOR CONTRIBUTIONS

Xu Yong and Huang Wenlin played a guiding role in carrying out the studies, collecting data, and drafting the manuscript. Huang Wenlin helped draft the man-

uscript. Xu Yong, Huang Wenlin, and Liu JinGe reviewed the manuscript.

REFERENCES

1. Chul Kim S, Kyoung Kwon S, Pyo Hong Y. Trends in the incidence of cryptorchidism and hypospadias of registry-based data in Korea: a comparison between industrialized areas of petrochemical estates and a non-industrialized area. Asian J Androl. 2011;13:715-8.
2. Schneuer FJ, Holland AJA, Pereira G, Jamieson S, Bower C, Nassar N. Age at surgery and outcomes of an undescended testis. Pediatrics. 2016;137:e20152768.
3. Hack WW, Sijstermans K, van der Voort-Doedens LM, Meijer RW, Haasnoot K. The high scrotal ("gliding") testis revised. Eur J Pediatr. 2007;166:57-61.
4. Thonneau PF, Gandia P, Mieusset R. Cryptorchidism: incidence, risk factors, and potential role of environment; an update. J Androl. 2003;24:155-62.
5. Baranzini SE, Mudge J, van Velkinburgh JC, et al. Genome, epigenome and RNA sequences of monozygotic twins discordant for multiple sclerosis. Nature. 2010;464:1351-6.
6. Elamo HP, Virtanen HE, Toppari J. Genetics of cryptorchidism and testicular regression. Best Pract Res Clin Endocrinol Metab. 2022;36:101619.
7. Menzies BR, Tarulli GA, Frankenberg SR, Pask AJ. Therian origin of INSL3/RXFP2-driven testicular descent in mammals. Front Cell Dev Biol. 2024;12:1353598.
8. Collet B, Desalegn AA, Swart K, et al. Anti-androgenic compounds in breast milk and cryptorchidism among Norwegian boys in the HUMIS birth cohort. Sci Total Environ. 2022;803:149746.
9. Seth A, Bournat JC, Medina-Martinez O, et al. Loss of WNT4 in the gubernaculum causes unilateral cryptorchidism and fertility defects. Development. 2022;149.
10. Langfelder P, Horvath S. WGCNA: an R package for weighted correlation network analysis. BMC Bioinformatics. 2008;9:559.
11. Staaf J, Glodzik D, Bosch A, et al. Whole-genome sequencing of triple-negative breast cancers in a population-based clinical study. Nat Med. 2019;25:1526-33.
12. Ritchie ME, Phipson B, Wu D, et al. limma powers differential expression analyses for RNA-sequencing and microarray studies. Nucleic Acids Res. 2015;43:e47.
13. Wu T, Hu E, Xu S, et al. clusterProfiler 4.0: A universal enrichment tool for interpreting omics data. Innovation (Camb). 2021;2:100141.
14. Cannistraci CV, Ogorevc J, Zorc M, Ravasi T, Dovc P, Kunej T. Pivotal role of the muscle-contraction pathway in cryptorchidism and evidence for genomic connections with cardiomyopathy pathways in RASopathies. BMC Med Genomics. 2013;6:5.
15. Jensen MS, Toft G, Thulstrup AM, et al. Cryptorchidism concordance in monozygotic and dizygotic twin brothers, full brothers, and half-brothers. Fertil Steril. 2010;93:124-9.
16. Urh K, Kunej T. Molecular mechanisms of cryptorchidism development: update of the database, disease comorbidity, and initiative for standardization of reporting in scientific literature. Andrology. 2016;4:894-902.
17. Bay K, Main KM, Toppari J, Skakkebæk NE. Testicular descent: INSL3, testosterone, genes and the intrauterine milieu. Nat Rev Urol. 2011;8:187-96.
18. Tai Y, Liu C, Yu S, et al. Gene co-expression network analysis reveals coordinated regulation of three characteristic secondary biosynthetic pathways in tea plant (Camellia sinensis). BMC Genomics. 2018;19:616.
19. Wang G, Yu J, Yang Y, et al. Whole-transcriptome sequencing uncovers core regulatory modules and gene signatures of human fetal growth restriction. Clin Transl Med. 2020;9:9.
20. Wu D, Smyth GK. Camera: a competitive gene set test accounting for inter-gene correlation. Nucleic Acids Res. 2012;40:e133.
21. Zhang Z, Chen L, Xu P, Xing L, Hong Y, Chen P. Gene correlation network analysis to identify regulatory factors in sepsis. J Transl Med. 2020;18:381.
22. Zhang J, Lan Q, Lin J. Identification of key gene modules for human osteosarcoma by co-expression analysis. World J Surg Oncol. 2018;16:89.
23. Ibrahim IM, Abdelmalek DH, Elfiky AA. GRP78: A cell's response to stress. Life Sci. 2019;226:156-63.
24. Mou L, Sun D, Qu J, et al. GRP78/IRE1 and cGAS/STING pathway crosstalk through CHOP facilitates iodoacetic acid-mediated testosterone decline. J Hazard Mater. 2024;476:135101.
25. Pakkasjärvi N, Taskinen S. Surgical treatment of cryptorchidism: current insights and future directions. Front Endocrinol (Lausanne). 2024;15:1327957.
26. Shaulian E, Karin M. AP-1 as a regulator of cell life and death. Nat Cell Biol. 2002;4:E131-6.
27. Martin LJ, Nguyen HT. Basic leucine zipper transcription factors as important regulators of Leydig cells' functions. Int J Mol Sci. 2022;23.
28. Song D, Lian Y, Zhang L. The potential of activator protein 1 (AP-1) in cancer targeted therapy. Front Immunol. 2023;14:1224892.
29. Mazzeo L, Ghosh S, Di Cicco E, et al. ANKRD1 is a mesenchymal-specific driver of cancer-associated fibroblast activation bridging androgen receptor loss to AP-1 activation. Nat Commun. 2024;15:1038.
30. Sakamoto T, Imai H. Hydrogen peroxide produced by superoxide dismutase SOD-2 activates sperm in Caenorhabditis elegans. J Biol Chem. 2017;292:14804-13.
31. Ceccanti S, Migliara G, De Vito C, Cozzi DA. Prevalence, management, and outcome of cryptorchidism associated with gastroschisis: A systematic review and meta-analysis. J

Pediatr Surg. 2022;57:1414-22.
32. Hemati U, Moshajari M, Jalali Mashayekhi F, Bayat M, Moslemi A, Baazm M. The effect of curcumin on NRF2/Keap1 signalling pathway in the epididymis of mouse experimental cryptorchidism. Andrologia. 2022;54:e14532.
33. Yu G, Liu X, Zhang D, et al. Zebrafish Nedd8 facilitates ovarian development and the maintenance of female secondary sexual characteristics via suppression of androgen receptor activity. Development. 2020;147.